DELPHI 97-111 CONF 93
28 July, 1997

Search for compositeness with leptonic, hadronic and photonic final states at LEP II energies

Preliminary

DELPHI Collaboration

F. Barão[1], M. Espirito Santo[1], P. Gonçalves[1], C. Matteuzzi[2], A. Onofre[1], R. Paiva[1], L. Peralta[1] and M. Pimenta[1]

[1] LIP-IST-FCUL, Av. Elias Garcia, 14, 1e, P-1000 Lisboa, Portugal

[2] INFN, Milan, Italy

Abstract

A search for compositeness with leptonic, hadronic and photonic final states has been made in data taken at LEP II by the DELPHI detector. The data analysed was accumulated at center-of-mass energies of 161 and 172 GeV and correspond to an integrated luminosity of about 20 pb^{-1}. Single and double production of excited leptons were investigated, and new particles were allowed to decay radiatively or through weak decays. A possible anomalous behaviour of the $e^+e^- \to \gamma\gamma(\gamma)$ process due to excited electron exchange in the t-channel was studied. A search for excited quarks singly produced and decaying into a quark plus a photon or a gluon is also reported. No signal of compositeness was found. Preliminary limits with 95% confidence level were derived on the masses and couplings of the composite states.

Paper submitted to the LP'97 Conference
Hamburg, July 28 - August 1st

1 Introduction

It is widely believed that Standard Model (SM), although extremely successful at the present energy scale, is not the final Theory. Many possible extensions of the SM discussed in the literature [1] predict the existence of new fermions.

This note updates the search for excited leptons reported by DELPHI at $\sqrt{s}$ = 161 GeV [2], combining it with the recent $\sqrt{s}$ = 172 GeV data and covers the searches for unstable excited quarks at centre-of-mass energies of $\sqrt{s}$ = 161 GeV and $\sqrt{s}$ = 172 GeV. The statistics corresponds to an integrated luminosity of 9.7 pb^{-1} and 10.1 pb^{-1} at $\sqrt{s}$ = 161 GeV and $\sqrt{s}$ = 172 GeV, respectively.

Excited fermions are expected in models with substructure in the fermionic sector. In this paper, following the simplest phenomenological models [3], excited fermions are assumed to have both spin and isospin 1/2 and to have both their LH and RH components in weak isodoublets (vector-like). Form factors and anomalous magnetic moments of excited fermions are not considered in the present analysis.

Previous limits set by DELPHI and by other experiments can be found in references [2] and [4].

2 Production and decay of excited fermions

2.1 Direct production

Excited fermions couple, according to their internal quantum numbers, to the photon and/or to the W and Z gauge bosons and thus can be pair produced at LEP. Excited fermion masses above $\sqrt{s}/2$ can be probed through the single production, depending on the scale Λ of the substructure.

In e^+e^- collisions the double production of charged excited fermions proceeds via s-channel γ and Z exchanges, while for excited neutrinos only the s-channel Z exchange contributes. Although t-channel contributions are also possible, they correspond to double de-excitation, and give a negligible contribution to the overall production cross-section [5].

For the single production, excited charged fermions can result from the s-channel γ and Z exchange while the excited neutrinos production modes depend on the relative strength of the couplings to both gauge bosons. Important additional contributions from the t-channel γ and Z exchange arise for the excited electron production while for the electronic excited neutrino the t-channel W exchange can be important [3, 5]. In the t-channel, the spectator charged lepton is emitted preferentially at low polar angle and often goes undetected in the beam pipe.

2.2 Indirect production

The process $e^+e^- \to \gamma\gamma(\gamma)$ can be used to probe compositeness at LEP and thus complement the excited electron direct searches for the mass region above the kinematical threshold.

The possible existence of a virtual excited electron mediating the $\gamma\gamma$ production diagrams could be seen as a modification on the angular distribution. This is usually parameterized as a modification to the lowest order differential cross section according to the expression [6],

$$\frac{d\sigma}{d\Omega} = \frac{\alpha^2}{s}\frac{1+cos^2\theta}{1-cos^2\theta}\left[1+\frac{1}{2}\left(\lambda\frac{s}{m_{e^*}^2}\right)^2(1-cos^2\theta)H(m_{e^*}^2, cos^2\theta)\right]$$

where

$$H(m_{e^*}^2, cos^2\theta) = a\left(a+\frac{1-cos^2\theta}{1+cos^2\theta}\right)\left[(1+a^2)-cos^2\theta\right]^{-1}$$

and

$$a = 2\frac{m_{e^*}^2}{s}$$

The cross section depends on the excited electron mass m_{e^*} and on the $ee^*\gamma$ coupling λ.

2.3 Decay mechanism

The effective electroweak Lagrangian [5] associated to magnetic transitions from excited leptons ℓ^* to ordinary leptons ℓ has the form

$$L_{\ell\ell^*} = \frac{1}{2\Lambda}\overline{f^*}\sigma^{\mu\nu}\left[gf\frac{\tau}{2}W_{\mu\nu}+g^{'}f^{'}\frac{Y}{2}B_{\mu\nu}+g_sf_s\frac{\lambda}{2}G_{\mu\nu}\right]f_L + h.c.$$

where Λ corresponds to the compositeness mass scale and the constants f, $f^{'}$ and f_s describe the effective changes from the SM coupling constants associated to the three gauge groups. The meaning of these couplings and of the other parameters is described in [5]. With the assumption $|f| = |f^{'}| = |f_s|$, the cross section depends simply on the parameter f/Λ, which is related to the excited fermion mass according to $f/\Lambda = \sqrt{2}\lambda/m_{f^*}$, where λ is the coupling of the excited fermion.

Decay Channel	M=80 GeV/c^2		M=170 GeV/c^2	
	$f=f^{'}$	$f=-f^{'}$	$f=f^{'}$	$f=-f^{'}$
$\ell^*\to\ell\gamma$	100	0	37	0
$\ell^*\to\ell Z$	0	0	9	36
$\ell^*\to\nu W$	0	100	54	64
$\nu^*\to\nu\gamma$	0	100	0	37
$\nu^*\to\nu Z$	0	0	36	9
$\nu^*\to\ell W$	100	0	64	54

Table 1: Branching ratios in % for excited lepton decays (upper part for excited charged leptons, lower part for excited neutrinos).

Excited fermions can decay by radiating a γ, a Z or a W. The decay branching ratios are functions of the f, $f^{'}$ and f_s coupling parameters of the model. Table 1 shows the branching ratios for some relevant values of f, $f^{'}$ and for two excited lepton mass values. For excited quarks, the gluon radiation transition is also possible becoming the most important decay mode. In fact, for excited quark masses around 160 GeV the gluon radiation mode accounts for more than 90% of the visible width.

For charged excited leptons, the electromagnetic radiative decay is forbidden if $f = -f^{'}$, and the decay then proceeds via three body decay modes through the Z and W bosons. If $f = +f^{'}$, the electromagnetic radiative decay branching ratio is close to 100% for m_{ℓ^*} below m_Z and m_W, and decreases to 37% for $m_{\ell^*} = 170$ GeV/c^2.

For excited neutrinos, the situation is reversed, so that the electromagnetic partial decay width is zero if $f = +f^{'}$. However, there is a significant contribution to the total decay width from the electromagnetic radiative decay if $f \neq f^{'}$, even if the difference $f - f^{'}$ is much smaller than f itself.

3 Final state topologies

The topologies that could result from the decay of unstable heavy fermions are quite diverse. The possible final states involve isolated leptons, isolated photons and the products of W and Z bosons decays, i.e., jets, leptons, missing energy ($\not{E}$) and missing momentum ($\not{p}$).

In this analysis, these topologies are classified as *leptonic* if they result from radiative decays of the heavy leptons or from W or Z leptonic decays and are classified as *hadronic* if they involve hadronically-decaying W or Z bosons.

The events can be characterized by the number of jets and the number of isolated leptons and photons. The different topologies will be referred to as $xijk$ according to the following rule: x is h or ℓ for *hadronic* or *leptonic* topologies and i, j, and k represent respectively the number of jets, the number of isolated charged particles, and the number of photons. As an example, h210 is an hadronic topology with two jets and one isolated lepton.

The criteria for isolated particles selection and jet clustering are explained in section 5, both for *hadronic* and *leptonic* events. For the moment, it should be mentioned that for *leptonic* events all charged particles are included in the jets and the concept of isolated leptons is not used.

In table 2 the relevant topologies for the different production and decay channels are shown. The topologies in brackets do not correspond directly to the physical final state but are often the observed ones. They become particularly important whenever there are particles produced with very low momentum or at very low polar angle. Empty entries in the table refer to channels in which no search is made.

Single and double photon final states arise in the case of a radiatively decaying excited neutrino.

4 The DELPHI detector and the data samples

A detailed description of the DELPHI apparatus and its performance can be found in [7]. This analysis relies both on the charged particle detection provided by the tracking system and the neutral cluster detection provided by the electromagnetic and hadronic calorimeters.

The main tracking detector is the Time Projection Chamber (TPC), which covers the angular range $20° < \theta < 160°$, where θ is the polar angle defined with respect to the

channel	topologies	
	single production	double production
$\ell^* \to \ell\gamma$	ℓ201,(ℓ101),(ℓ102)	ℓ202
$\ell^* \to \nu W$	h210,(h200),ℓ200	h210,h400
$\ell^* \to \ell Z$	h220,(h210),ℓ400	-
$\nu^* \to \nu\gamma$	ℓ001	ℓ002
$\nu^* \to \ell W$	h210,(h200),ℓ200	h230,(h210),h420,(h400)
$\nu^* \to \nu Z$	h200,ℓ200	-
$q^* \to qg$	h300	-
$q^* \to q\gamma$	h201, (h101)	-
$q^* \to q'W$	h210	-
$q^* \to qZ$	h200,h220	-
$e^+e^- \to \gamma\gamma$	ℓ002	

Table 2: Observable topologies corresponding to the different production and decay modes of excited fermions.

beam direction. Other detectors contributing to the track reconstruction are the Vertex Detector (VD), the Inner and Outer Detectors, the Forward Chambers, and the Muon Chambers. The best momentum resolution obtained for muons is $\sigma(1/p) = 0.57 \times 10^{-3}$ (GeV/c)$^{-1}$. The VD consists of three cylindrical layers of silicon strip detectors, each layer covering the full azimuthal angle. The polar angle coverage of the vertex detector was increased down to 25° in 1996.

The barrel electromagnetic calorimeter (HPC) and the forward electromagnetic calorimeters (FEMC and STIC) are used for the reconstruction of electromagnetic showers. The STIC (Small angle TIle Calorimeter), which is the DELPHI luminosity monitor, was used for electromagnetic shower detection at very low polar angle and has an energy resolution of 2.7% for 45 GeV electrons. The energy resolutions of the HPC (High density Projection Chamber) and FEMC (Forward Electromagnetic Calorimeter) calorimeters are parameterized respectively as $\sigma(E)/E = 0.043 \oplus 0.32/\sqrt{E}$ and $\sigma(E)/E = 0.03 \oplus 0.12/\sqrt{E} \oplus 0.11/E$, where E is expressed in GeV and the symbol '$\oplus$' implies addition in quadrature. The hadron calorimeter covers both the barrel and forward regions. It has an energy resolution of $\sigma(E)/E = 0.21 \oplus 1.12/\sqrt{E}$ in the barrel and about $2/\sqrt{E}$ in the forward region.

Photon detection in the region between the barrel and the forward electromagnetic calorimeters (polar angles around 40° and 140°) is achieved using the information of a set of scintillator counters (40° taggers). The efficiency of the taggers was checked with Bhabha events and found to be greater than 95%.

Except for purely photonic events, discussed in sections 5.3 and 6.2, the trigger efficiency is very close to 100%.

The effects of the experimental resolution, both on the signals and on the backgrounds, were studied by generating Monte Carlo events for the SM background processes and for the possible signals and passing them through the full DELPHI simulation and reconstruction chain.

Bhabha events, $e^+e^- \to Z\gamma$, $e^+e^- \to WW$, $e^+e^- \to We\nu$, $e^+e^- \to ZZ$, and $e^+e^- \to Zee$, events were generated with PYTHIA [8]. In all four-fermion channels, studies with the EXCALIBUR generator [9] were also performed. The two-photon ("$\gamma\gamma$") physics events were generated according to the TWOGAM [10] generator for quark channels and the Berends, Daverveldt and Kleiss generator [11] for the electron, muon and tau channels. Compton events were generated according to [12], $e^+e^- \to \gamma\gamma$ events according to [13], and the single photon events from the process $\nu\bar{\nu}\gamma$ were generated with NUNUGPV, based in the calculation in [14].

Single and double excited fermion events were generated according to the cross-sections defined in [5] involving γ, Z and W exchange. The hadronization and decay processes were simulated by JETSET 7.4 [8]. The initial state radiation effect was included at the level of the generator for the single production, while for the double production it was taken into account in the total cross section. All the possible decay modes were included in the simulation.

5 Event Selection

The basis of event selection and classification is as follows. A visible energy greater than $0.2\sqrt{s}$ in the polar angle region between 20° and 160° was required, including at least one particle with an energy greater than 5 GeV. In fact, in all the relevant topologies energetic visible particles are present. Furthermore, these particles are produced isotropically close to the kinematical limit. In this way the "$\gamma\gamma$" background is drastically suppressed.

Events with measured charged or neutral particles having energy greater than $\sqrt{s}$ were rejected. In addition, at least one charged particle in the polar region between 25° and 155° with associated hits in the vertex detector was required. These criteria are useful in rejecting cosmic rays background.

To be considered, a charged particle had to have a momentum greater than 0.4 GeV/c, a polar angle between 20° and 160°, and a track length greater than 30 cm. In the central region ($40° < \theta < 140°$), the impact parameters in the transverse plane and in the beam direction had to be below 5 cm and 10 cm respectively. These values were increased to 10 cm and 20 cm in the forward region ($20° < \theta < 40°$ or $140° < \theta < 160°$). Events were classified as *hadronic* if there were at least eight detected charged particles and as *leptonic* otherwise.

Charged particles were considered isolated if, in a double cone centered on their track with internal and external half angles of 3° and 15°, the total energy deposited was less than 1 GeV. Inside the inner cone, all the clusters and tracks were considered to be associated, and the total energy had to be greater than 5 GeV. In all hadronic topologies with isolated leptons, these were required to have associated hits inside a two degrees cone in at least two layers of the vertex detector.

Isolated charged particles with an associated electromagnetic energy greater than 20% of their momentum were loosely identified as electrons. Isolated particles were classified as muons by requiring an electromagnetic energy lower than 20% of its momentum and at least one associated hit in the muon chambers.

In the *hadronic* and *leptonic* topologies neutral clusters were considered to be photons if they had no associated hits inside a two degrees cone in more than one layer of the vertex detector and, if hadronic energy was present, they had at least 90% of this energy deposited in the first layer of the hadronic calorimeter.

Photons were considered to be isolated if, in a double cone centered in the cluster and having internal and external half angles of 5° and 15°, the total energy deposited was less than 1 GeV. Inside the inner cone, all the clusters were considered associated, no charged particles were allowed, and the total energy had to be greater than 5 GeV.

In all the studied topologies, it was required that at least one of the detected photons was above 10° in polar angle and had an energy greater than 10 GeV.

All the events were clustered into jets using the Durham jet algorithm [15]. In this algorithm, a resolution variable

$$y_{ij} = 2\min(E_i^2, E_j^2)/E_{vis}^2 \cdot (1 - \cos\theta_{ij})$$

is computed for all pairs of particles. $E_{i,j}$ are the energies of the particles, θ_{ij} is their opening angle, and E_{vis} is the visible energy in the event. The pair for which y_{ij} is smallest is replaced by a pseudoparticle with four-momentum equal to the sum of their four-momenta. In this analysis, the algorithm is used in two different ways:

- the procedure is iterated until all pseudo-particle pairs have a y_{ij} larger than a certain y_{cut} value. A cut-off value of y_{cut}=0.003 was used. This relatively low value of y_{cut} is well suited to look for topologies with many jets.

- the procedure is iterated until all particles are clustered into a certain fixed number of jets (N_{jets}). In this case the value of the resolution variable y at the last iteration, $y_{cut(N_{jets}+1 \to N_{jets})}$, allows a better characterization of the event topology.

For *hadronic* events, all neutral and charged particles not associated to isolated leptons and photons were included in the jets. The algorithm was applied three times, requiring N_{jets}=2, 3 and 4. In order to increase the purity of the 2-jets event sample, only events with $y_{cut(3\to2)}$ <0.06 were kept. Identically, for the 3-jets events the y_{cut} variables were constrained to $y_{cut(3\to2)} > 0.003$ and $y_{cut(4\to3)} < 0.001$. For a similar reason, in the 4-jets event sample only the events with a charged multiplicity normalized to its mean value greater than 1.1 were retained.

For the *leptonic* events, only the isolated photons were left out of the jets. Charged particles are treated not as isolated objects but as low multiplicity jets. This accounts for the fact that taus can decay into several charged and neutral particles and electrons can be accompanied by other electrons and photons due to interactions with matter. However, to avoid clustering several isolated leptons in the same jet, the number of jets was forced to be at least equal to the number of isolated charged particles found previously. Furthermore, for the ℓ200 topology, where forward Bhabha events are dominant, it was required that at least one of the jets had been previously identified as an isolated lepton.

The jets in *leptonic* events were loosely identified as electrons or muons according to the criteria described for isolated leptons. For a jet to be identified as a muon, it was also required that it did not contain more than two tracks.

Jets were considered charged if they contained at least one charged particle. Only events with all jets classified as charged and with axis in the polar region between 20° and 160° were kept.

5.1 Selected *hadronic* events

5.1.1 Single production topologies

In *hadronic* events from single excited leptons production, the jets originate from the decay of a W or a Z which is not produced at rest. Candidate events should have two charged jets with high acollinearity (A_{col}) and acoplanarity (A_{cop}) [1], and the two-jet system must have a high mass (M_{jj}) and a high momentum (P_{jj}). The main backgrounds for these topologies are $e^+e^- \to q\bar{q}(\gamma)$ events, including radiative returns to the Z ($e^+e^- \to Z\gamma$) where the photon was lost in the beam pipe, and semileptonic decays of W pairs. In the first case the events are characterized by two collinear and/or coplanar jets. In addition, radiative return events have a high missing momentum at very low polar angle. The WW background events have simultaneously an energetic lepton and an appreciable amount of missing energy.

Hadronic events from single excited quark production are characterized by the presence of three jets (h300) in the case of the decay through the gluon and by one energetic photon with a large isolation angle ($\mathrm{A}^{\gamma}_{iso}$) and two jets (h201) in the case of the electromagnetic radiative decay. The main backgrounds for these topologies are $e^+e^- \to q\bar{q}(\gamma)$ events and hadronic decays of W pairs.

Near the kinematic limit the spectator quark is essentially produced at rest and the observed topologies are then h200 and h101. While the h101 corresponds to a very clear signature in the h200 the SM $q\bar{q}$ events constitute an enormous and irreducible background.

In order to improve the estimation of the momentum and energy of the jets a kinematic constraint fit was applied to the selected events. The constraints imposed depend on the particular final state in study. In all the relevant *hadronic* final states where the jet pair comes from the decay of W or Z bosons, the invariant mass of the two-jet system was constrained to be either m_W or m_Z. Since the h210 topology can arise from both the W and the Z channel (see table 2) the fit was performed twice for this topology, using m_W and m_Z. If there are no undetected particles, as it is the case for the h201 and h300 topologies, energy and momentum conservation can be imposed. The input quantities for the fit were the measured vector momenta of the objects. The details of the fitting procedure, namely the errors on the input variables, can be found in reference [16].

The main selection criteria for the different topologies are summarized in table 3. The number of constraints imposed for each topology is also given in the table. In all cases, only events with a χ^2 (per degree of freedom) lower than 5 were retained.

The selection criteria involving the mentioned variables allow a quite efficient background rejection. The cut values were tuned for each topology in order to optimize the signal to noise ratio. For the h200 topology, events with signal in more than two 40° taggers inside a 20° cone centered in the direction of the missing momentum were rejected. This criterion is useful in rejecting $q\bar{q}\gamma$ events in which the photon was lost in the region between the electromagnetic calorimeters.

5.1.2 Double production topologies

The relevant topologies for the double production of charged excited leptons are characterized by two jets and one isolated lepton or by four jets. In the case of excited neutrinos,

[1] The acoplanarity is defined as the acollinearity in the plane perpendicular to the beam.

	selection variables			
topol	**angles**	**invariant masses**	**other criteria**	**fit**
h300	$\min(A^{jj}) > 40°$			4C
h200	$A^{jj}_{col} > 50°$ $A^{jj}_{cop} > 25°$ $\not\theta > 25°$	$M_{jj} > 40\mathrm{GeV/c^2}$		
h210	$A^{jj}_{col} > 40°$ $A^{jj}_{cop} > 15°$ $\not\theta > 20°$		$[p_\ell < 25GeV/c, \not p > 25GeV/c]$ or $[p_\ell > 40GeV/c, \not p < 30GeV/c]$	1C
h220	$A^{jj}_{col} > 20°$ $A^{jj}_{cop} > 10°$ $\not\theta > 20°$	$M_{jj} > 40\mathrm{GeV/c^2}$		5C
h201	$A^{\gamma}_{iso} > 25°$ $\theta_\gamma \in [40°, 140°]$		$E_\gamma > 20$ GeV	4C
h101	$A^{j\gamma}_{col} < 30°$ $\theta_\gamma \in [40°, 140°]$		$E_\gamma > 30$ GeV	4C

Table 3: Selection criteria for single production *hadronic* topologies.

additional leptons are present in the final state. However, near the kinematical limit, these leptons can be clustered in the jets due to their low momenta. For this reason, the most relevant topologies will still be h210 and h400. In this channels there is a nearly irreducible background from WW events.

The kinematic fit constraining the di-jet masses (see section 5.1.1) was applied to these topologies. In the four jets topology energy-momentum conservation was also required. Events with a good χ^2 value were rejected. This cut is efficient in rejecting WW background.

Two jets and one isolated lepton topology

The specific selection criteria for the charged excited leptons channel in the topology with two jets and at least one isolated lepton were that:

- the measured invariant mass of the two jets had to be between 20 GeV/c^2 and 70 GeV/c^2,
- the momentum of the isolated particle had to exceed 20 GeV/c and its angle to the nearest jet had to be above 45°,
- the missing momentum had to be greater than 20 GeV/c,
- the ratio between the missing momentum and the missing energy had to be lower than 0.7,
- the χ^2 value had to be greater than 1.

The same set of cuts was applied in the excited neutrinos search if only one isolated lepton was found in the final state. If more than one lepton is present, background problems are reduced and the selection criteria could be simplified:

- the measured invariant mass of the two jets had to be greater than 25 GeV/c^2,
- the ratio between the missing momentum and the missing energy had to be lower than 0.7.

Four jets topology
The basic selection criteria for the charged heavy lepton candidates in the four jets topology were that:

- the lowest jet-jet invariant mass and jet-jet angle exceeded 20 GeV/c^2 and 55° respectively,
- the missing energy was greater than 40 GeV,
- the polar angle of the missing momentum was between 20° and 160°,
- the ratio between the missing momentum and the missing energy was lower than 0.6,
- The angle between the missing momentum and the axis of the closest jet exceeded 15°,
- the χ^2 value was greater than 5.

The same set of cuts was applied in the excited neutrinos search if no isolated leptons were found in the event. If one or more isolated leptons were found, the selection criteria could be simplified:

- the lowest jet-jet invariant mass had to exceed 20 GeV/c^2,
- the ration between the missing momentum and the missing energy had to be lower than 1,
- the χ^2 had to be greater than 8.

5.2 Selected *leptonic* events

Events classified as *leptonic* can be originated from radiative decays of excited leptons, in which case there will be photons in the final state, or from decays into W or Z bosons decaying into leptons, in which case there will be only leptons (treated as low multiplicity charged jets, as explained above) involved (see table 2). The two analysis are quite different and will be treated separately.

5.2.1 *leptonic* events without isolated photons

In the case of a singly produced excited leptons decaying via a W, the signal events are characterized by the presence of two acoplanar jets and missing energy ($\ell200$ topology in table 2). The background for this topology comes essentially from $e^+e^- \rightarrow \ell^+\ell^-(\gamma)$ processes, in particular Bhabha events where the photon was lost, and from leptonic decays of W pairs. In the WW background, both the charged jets come from W decays, having a large momentum. The selection criteria were the following:

- $\mathrm{A}_{col} > 40°$,
- $\mathrm{A}_{cop} > 25°$.

For charged excited leptons, there is a large asymmetry between the momenta of the jets and an additional cut was applied:

- $\mathrm{p}_2 < 30\mathrm{GeV/c}$.

In the case of a singly produced excited lepton decaying into leptons via a Z boson, the signal events are characterized by the presence of four charged jets ($\ell400$ topology). Two of the jets result from the Z decay and thus have a large invariant mass while the second pair of jets has a low invariant mass.

The background for this topology comes from 4-fermion processes. In this analysis it is required that at least three of the jets have been previously identified as isolated leptons in order to avoid hadronic contamination.

5.2.2 *leptonic* events with isolated photons

Final states resulting from singly produced excited charged leptons decaying radiatively are characterized by an energetic photon with an isotropic polar angle distribution and two charged particle jets ($\ell201$ topology). Near the kinematic limit one of these jets will not be observed due to its low momentum ($\ell101$ topology). This final state topology is particularly relevant when the t-channel cross section dominates (e^* single production) and the spectator lepton is frequently lost in the beam pipe. For this specific case the $\ell102$ topology, in which one of the jets is at very low polar angle and was misidentified as a photon, also becomes useful.

The main background for the $\ell201$ topology comes from $e^+e^- \rightarrow \ell^+\ell^-$ radiative events. Those having a photon emitted at very low polar angle or with low energy are easily eliminated. However, events with a hard isolated photon constitute an irreducible background.

For the $\ell101$ and $\ell102$ topologies, the background comes from Bhabha events with one electron lost or misidentified as a photon, and from Compton events. In Bhabha events, there are two essentially back to back particles in the forward region of the detector. In Compton events the charged jet and the photon are acollinear and there is a large amount of energy deposited in the forward part of the detector.

Final states resulting from doubly produced excited charged leptons decaying radiatively are characterized by the presence of two charged jets and two hard photons in the detector. In these events there must be two lepton-photon combinations with compatible invariant masses. Possible background comes from doubly radiative $e^+e^- \rightarrow \ell^+\ell^-$ events.

In three- or four-body topologies, as stated in [2], the energies can be rescaled by imposing energy and momentum conservation and using the polar and azimuthal angles, which are well measured in the detector. This procedure can significantly improve the energy resolution. The compatibility of the momenta calculated from the angles with the measured momenta was quantified on a χ^2 basis[2] For two-body topologies, the same method can be applied assuming the presence of a third particle along the beam direction.

Only events with $\chi^2 < 5$ either for photons or for charged particles were kept. The fact that the condition $\chi^2 < 5$ was not applied simultaneously to the photons and to the charged particles allows events in the electron and muon channels with photons near the borders of the calorimeter modules (where electromagnetic energy can be badly reconstructed) to be kept. Concerning the tau channel, it should be noted that the rescaling procedure can still be applied because the charged decay products essentially follow the direction of the primary tau. However, due to the neutrinos, the rescaled momentum of the charged jet are expected to be substantially different from the measured one. In addition to this criteria, the events selected in all channels were checked for their coplanarity (the sum of the angles between the particles had to be greater than 355°).

	selection variables		
topology	**jet variables**	**photon variables**	**angles**
ℓ201 e	$p_{jet_1} > 10$GeV/c	$\theta_\gamma > 40°$	-
ℓ201 μ		-	-
ℓ201 τ	-	$\theta_\gamma > 20°$	-
ℓ101 e	$p_{jet} > 10$GeV/c	$p_\gamma > 40$GeV/c $\theta_\gamma > 40°$	$100° < A^{j\gamma} < 179°$
ℓ101 μ			-
ℓ101 τ			$100° < A^{j\gamma} < 179°$
ℓ102 e	$p_{jet} > 10$GeV/c	$\theta_{\gamma_1} > 40°$ $\theta_{\gamma_2} < 20°$	$15° < A^{j\gamma} < 179°$
ℓ202 e	$p_{jet_1} > 10$GeV/c $p_{jet_2} > 10$GeV/c	$p_{\gamma_1} > 20$GeV/c	-
ℓ202 μ		-	-
ℓ202 τ	-	$p_{\gamma_1} > 20$GeV/c	-

Table 4: Selection criteria for *leptonic* topologies with isolated photons.

The backgrounds and efficiencies depend significantly, for these topologies, on the flavour of the final state leptons involved. Thus, different selection criteria are used for the different flavors. The main selection criteria are summarized in table 4.

For the ℓ101 topology, an additional cut was applied in the electron channel: events that, after the rescaling procedure, had more than 30 GeV/c assigned to the particle lost along the beam direction were rejected. This criterion is useful to eliminate Compton events.

[2] the χ^2 parameter was defined separately for charged jets ($\chi^2_{charged}$) and photons ($\chi^2_{photons}$) as $\chi^2 = \frac{1}{n}\sum_{i=1,n}\left(\frac{p_i^{calc} - p_i^{meas}}{\sigma_i}\right)^2$ where n is the number of measured particles, p_i^{meas} is the measured momentum or energy and p_i^{calc} is the momentum calculated from the kinematic constraints. For the definition of the error σ_i and more details see the DELPHI publication on $\sqrt{s}$=130-136 GeV results in reference [2].

In the $\ell202$ topology only events having both photons with an energy greater than 10 GeV and above $10°$ in polar angle are kept.

5.3 Selected photonic events

Neutral excited leptons can give rise to single or two-photon events depending how their production occur. Thus, excited neutrinos produced in pairs and decaying radiatively to a photon plus an ordinary neutrino are tagged through the $\ell002$ topology and those which are produced singly will be detected with the $\ell001$ topology. The SM processes constituting background to both topologies are essentially radiative Bhabhas, Comptons, QED $e^+e^- \to \gamma\gamma$ and $e^+e^- \to Z\gamma(\gamma)$ with $Z \to \nu\nu$.

In order to reduce drastically the Bhabha and Compton background, single gamma events were required to have polar angles above $45°$ and no other electromagnetic energy deposition was allowed out of a $20°$ cone. Besides, it was demanded that the photons have a line of flight compatible within $15°$ with the shower direction reconstructed by the HPC calorimeter. A selection criteria based on HCAL has been applied to veto cosmics.

The two-photon sample was selected requiring at least two photons obeying to the following criteria:

- Energy greater than 25% of the centre-of-mass energy in the polar region between $25°$ and $155°$.
- At least three HPC layers with more than 5% of the total electromagnetic energy, for the HPC energy depositions not pointing to the ϕ intermodular zones.

Furthermore, the hadronic energy is required to be less than 15% of the total deposited energy unless the photon falls in the HPC ϕ cracks, in which case it is demanded that the HCAL first layer energy deposition is greater than 90% of the total photon energy.

The $\gamma\gamma$ sample was enriched through the recovery of photons converted after the VD detector. The number of converted photons was limited to one per event and their recovering was performed in a slightly reduced geometrical acceptance ($\theta > 30°$), in order to keep a high level background rejection. An unconverted photon is defined as an energy deposition with no charged tracks and no VD track element associated within $2°$ and $6°$ for the barrel ($\theta > 40°$) and the forward ($\theta < 35°$) regions, respectively. A VD track element is defined by at least two $R\phi$ hits on different layers with a tolerance of 0.5 degrees.

5.4 Event flavour identification

The event flavour, in the *hadronic* topologies with isolated leptons, was tagged by loosely identifying the leptons according to the criteria described in section 5.

The flavour identification for *leptonic* topologies was performed using the charged jets identification and, whenever possible, the comparison between the measured momenta and the momenta computed using the rescaling procedure (see section 5.2.1).

In the *leptonic* topologies with no isolated photons, the rescaling procedure is not applied, since there are always at least two neutrinos involved. There is also at least one charged jet coming from the decay of a W or Z boson and containing no relevant flavour information. Events are classified as electron or muon events whenever the lowest energy jet was identified as such. All events are kept in the tau channel.

In the topologies involving isolated photons, either there are no missing particles or there is only one particle lost along the beam pipe and the momenta can be computed imposing energy-momentum conservation. Events were kept as candidates in the electron (muon) channel if at least one of the jets was identified as an electron (muon) and no jets were identified as muons (electrons) and if $\chi^2_{charged} < 5$. For the $\ell 101$ topology, where background problems are more severe, it was also required that $\chi^2_{photons} < 5$. Events were kept as candidates in the tau channel if $\chi^2_{charged} > 5$ and $\chi^2_{photons} < 5$.

6 Results

6.1 Events with jets and leptons

The present section discusses the results obtained at $\sqrt{s} = 161$ GeV and $\sqrt{s} = 172$ GeV on both the single production of excited quarks and the double production of excited leptons. Single production of excited leptons at $\sqrt{s} = 172$ GeV is also presented. The results related to the single production of excited leptons at $\sqrt{s} = 161$ GeV were reported in a recent DELPHI publication [2] but have been taken into account in section 7 for the limits calculation.

The number of candidates at different selection levels is given in tables 5 and 6 for *hadronic* and *leptonic* topologies respectively. Selection level 1 corresponds to the general criteria, before any specific topology cuts (section 5); Level 2 corresponds to specific topology cuts, without flavour tagging (sections 5.1 and 5.2). In level 3 flavour tagging is included (section 5.4). The numbers in brackets give the SM expectations. In the different selection levels and topologies, a fair agreement between data and MC expectations is found. It should be noted that whenever the same topology is considered twice in the table (W and Z decay for the h210 topology, charged and neutral case for the double production topologies) the selections are not exclusive. For this reason, there is an overlap between the events selected in both cases.

Data and SM simulation distributions at $\sqrt{s}$ =172 GeV for the *hadronic* topologies at selection level 1 are shown in Figure 1. 1(a) and 1(b) show, respectively, the jet-jet acollinearity and the jet-jet invariant mass for the h200 topology. In 1(c) the isolation angle of the lepton in the h210 topology is shown. Figure 1(d) concerns the h400 topology and shows the largest jet-jet invariant mass. There is, for all the distributions, a reasonable overall agreement.

In figure 2 distributions concerning the $\ell 201$ topology are shown. Figure 2(a) shows the invariant mass for the lepton-lepton pairs using the momenta calculated from the kinematic constraint. The two possible $\ell\gamma$ invariant mass combinations are plotted in Fig. 2(b). Figure 2(c) presents the energy and Fig. 2(d) represents the isolation angle of the radiated photon. There is a good agreement between the data and SM simulation.

Figure 3 shows the distributions of the jet-pair invariant mass (a) and of the jet-photon pair invariant mass for the two possible combinations (b) existing on the h201 topology. For the h300 topology, the distributions of the lowest jet isolation angle and of the highest jet-jet invariant mass are shown in 3(c) and 3(d) respectively. In all the figures, a fair agreement between data and the SM prediction is observed.

The excited fermion mass can be, in many topologies, estimated from the momenta and directions of final state particles. Relevant cases are the $\ell\gamma$ and jet-γ and jet-jet

$\sqrt{s}$	topology	selection level				
		1	2	3		
				e	μ	τ
161 GeV	h300	$768(753 \pm 14)$	$29(30 \pm 2)$	-	-	-
	h201	$345(288 \pm 7)$	$39(44 \pm 3)$	-	-	-
	h101	$4(1.4 \pm 0.5)$	$1(0.8 \pm 0.3)$	-	-	-
172 GeV	h300	$679(660 \pm 11)$	$27(24 \pm 2)$	-	-	-
	h200	702(696±7)	0(2.7±0.3)	-	-	-
	h210 W	66(55±2)	5(2.4±0.2)	3(1.2±0.2)	1(0.8±0.1)	5(2.4±0.3)
	h210 Z	66(55±2)	5(2.0±0.2)	3(1.1±0.2)	1(0.7±0.1)	5(2.1±0.3)
	h220	2(2.8±0.3)	0(0.12±0.04)	0(0.07±0.04)	0(0.02±0.01)	0(0.12±0.04)
	h201	$240(214 \pm 4)$	$36(33 \pm 2)$	-	-	-
	h101	$5(0.7 \pm 0.2)$	$0(0.3 \pm 0.1)$	-	-	-
172 GeV	h400 char	99(111±3)	2(2.7±0.6)	-	-	-
	h4X0 neut		2(3.9±0.7)	-	-	-
	h210 char	52(38±2)	2(4.0±0.8)	-	-	-
	h2X0 neut		3(4.4±0.8)	-	-	-
161 GeV	h400 char	84(92±4)	0(1.4±0.4)	-	-	-
	h4X0 neut		1(2.2±0.5)	-	-	-
	h210 char	35(27±2)	1(1.5±0.3)	-	-	-
	h2X0 neut		1(2.0±0.4)	-	-	-

Table 5: Number of selected events for *hadronic* topologies. The numbers in brackets are the simulation expectations. The topologies below the double line correspond to the double production case.

invariant masses, the jet-jet-lepton invariant mass and the recoil mass of isolated leptons. Signal simulation studies allowed us to determine the mass resolution for each situation.

In *leptonic* events, the mass resolution of the lepton-photon pair, after applying the kinematic constraints, was found to be about 1 GeV/c^2 for electrons and muons and about 2 GeV/c^2 for taus.

In *hadronic* events with one isolated lepton, the resolution on the lepton recoil mass ($m_\ell^2 = s - 2\ k\ P_\ell \sqrt{(s)}$, where k is 1.0 for electrons and muons and 1.4 for taus to take in account the missing energy in tau decay) is about 1 GeV/c^2 for muons, 1.5 GeV/c^2 for electrons and 2.5 GeV/c^2 for taus. The resolution on the jet-jet-lepton invariant mass is about 5 GeV/c^2 for e and μ and 15 GeV/c^2 for τ. The resolution on the jet-photon invariant mass is about 2 GeV/c^2. The same is true for the jet-jet invariant mass in the h300 topology.

topology	selection level 1	2	3
ℓ201 e	47(44±2)	15(17±1)	6(10.3±1.3)
ℓ201 μ		27 (37±2)	5(5.0±0.4)
ℓ201 τ		20 (29±2)	6(4.2±0.6)
ℓ101 e	79(71±5)	2 (3.1±0.7)	0(1.0±0.5)
ℓ101 μ		11 (15±2)	2(0.3±0.1)
ℓ101 τ		6 (11±2)	3(0.4±0.2)
ℓ102 e	22(17±2)	3 (3.2±1.0)	3(3.2±1.0)
ℓ200 e	1200(1159±14)	1 (3.7±0.4)	0(2.4±0.3)
ℓ200 μ			1(0.7±0.1)
ℓ200 τ			1(3.7±0.4)
ℓ200 ν_e		6 (7.7±0.7)	3(4.7±0.7)
ℓ200 ν_μ			3(1.9±0.2)
ℓ200 ν_τ			6(7.7±0.7)
ℓ400	1(0.2±0.1)	1 (0.12±0.04)	1 (0.12±0.04)
ℓ400			1 (0.12±0.04)
ℓ400			1 (0.12±0.04)
ℓ202 e	4(1.4±0.2)	1 (0.3±0.1)	0 (0.03±0.03)
ℓ202 μ		1 (0.3±0.1)	1(0.2±0.1)
ℓ202 τ		1 (0.3±0.1)	1(0.3±0.1)

Table 6: Number of selected events for *leptonic* topologies. The numbers in brackets are the simulation expectations.The topologies below the double line correspond to the double production case.

6.2 Events with only photons

In the single photon channel (ℓ001), only events with $E_\gamma > 25$ GeV and a polar angle of $45° < \theta < 135°$ were retained. A total number of 7 candidates passed these selection criteria. The events must be corrected for the trigger and identification efficiencies. The latter depends on the photon energy but is practically constant and equal to 78% for photon energies above 25 GeV. The trigger efficiency has been measured with radiative ($\mu\mu\gamma$ and $ee\gamma$) and Compton events. In the HPC it shows to be strongly dependent with the photon energy up to around 12 GeV, ranging from 65% at 25 GeV to 90% for $E_\gamma > 40$ GeV approximately. These numbers have a drop of about 50% in the second period of the $\sqrt{s}$ =172 GeV run due to a problem at present still under investigation.

The main source of background for the single gamma channel is the QED process $e^+e^- \rightarrow \gamma e^+e^-$ where the two electrons escape undetected along the beam pipe. This process has a very high cross section, decreasing rapidly when E_γ and the photon polar angle increase. In the energy and angular region considered here, the expectation from the QED process and other backgrounds, such as beam gas, "$\gamma\gamma$" collisions, $e^+e^- \rightarrow \gamma\gamma$, cosmic and Compton events were found to be negligible. After correcting for backgrounds and efficiencies, the measured cross section inside the acceptance defined above was found to be

$$\sigma(e^+e^- \rightarrow \gamma + invisible\, particles) = 1.1 \pm 0.4 \pm 0.1\ pb$$

where the first quoted error is statistical and the second one is systematic. The systematic error comes mainly from the errors on the detection efficiencies and the calorimeter energy scale. The SM prediction for $e^+e^- \rightarrow \gamma Z^0$ with $Z^0 \rightarrow \nu\overline{\nu}$ is expected to be 1.7 pb.

In the present analysis signal events would be characterized by the presence of a very energetic photon. No events were found with a single photon having E_γ >75 GeV in the barrel region. From the SM reaction $e^+e^- \rightarrow \gamma\nu\overline{\nu}$ 0.02 $\pm$ 0.01 events were expected.

In the two photon channel (ℓ002), the two photons must have high energy and can be very acollinear and acoplanar in the case of the double excited neutrino production or be essentially collinear in the case of the QED $e^+e^- \rightarrow \gamma\gamma$ process mediated by an excited electron. For the acollinear sample the analysis presented in [17] was used. Two events with an acoplanarity greater than 10° were found at $\sqrt{s}$ = 172 GeV while 0.18 $\pm$ 0.01 events were expected from the QED background reaction $e^+e^- \rightarrow \gamma\gamma$ and 0.81 ± 0.03 from the process $e^+e^- \rightarrow Z\gamma\gamma$ with the Z decaying into neutrinos.

For the $\gamma\gamma$ collinear sample, events having photons with an energy greater than 1/3 of the beam energy and an acollinearity lower than 30° were selected. The number of events that passed these criteria in the total sample including the two center-of-mass energies was 92 to be compared with 89 ± 2 from the QED $e^+e^- \rightarrow \gamma\gamma$ process. The contribution from the Compton and Bhabha channels was estimated as negligible. The mean trigger efficiency was found to be 85%.

Using this total sample the total cross section at an average center-of-mass energy of $<\sqrt{s}>$=166.7 GeV inside the fiducial region defined in section 5.3 could be computed. Since this is to be compared with the lowest order QED prediction for $e^+e^- \rightarrow \gamma\gamma$, as explained in section 2.2, a radiative correction factor computed using the MC generator of Berends and Kleiss [13] was applied to the measured value. A cross section of σ_0 = 8.18 ± 0.85 pb was obtained, in very good agreement with the QED prediction of 8.17 pb.

7 Limits

The search for the production of excited fermions involves many final states. The relevance of the different final states depends, as discussed in section 2.3, on the decay branching ratios which are functions of the excited fermion mass and of the coupling parameters.

The numbers of excited fermion candidates, as well as the SM expectations, are summarized in table 7 as a function of the excited fermion type and decay mode, for single production. The number of candidates selected from data and simulation at $\sqrt{s}$=172 GeV and $\sqrt{s}$=161 GeV are summarized in table 8 for double production modes.

The possible excited fermion masses can be deduced in most of the topologies, as referred to in the previous section. Events in which the fermion mass could not be estimated were treated as candidates for all the mass values.

The efficiencies, including the trigger efficiency, are given in tables 9 and 10 for chosen fermion mass values in all the studied channels. For excited leptons, the dependence of the efficiency on the mass is weak, because of the combination of the several topologies studied. For excited quarks decaying in quark-gluon the efficiency slowly decreases from

$\sqrt{s}$	channel	e	μ	τ
172	$\ell^* \to \ell\gamma$	9(15±2)	7(5.3±0.4)	9(4.6±0.6)
GeV	$\ell^* \to \nu W$	3(3.9±0.4)	1(3.5±0.3)	5(5.1±0.4)
	$\ell^* \to \ell Z$	4(1.3±0.2)	2(0.8±0.1)	6(2.3±0.3)
172	$\nu^* \to \nu\gamma$	0(0.02±0.01)		
GeV	$\nu^* \to \ell W$	3(7.3±0.4)	3(3.5±0.4)	5(5.1±0.4)
	$\nu^* \to \nu Z$	0(2.7±0.3)	0(2.7±0.3)	0(2.7±0.3)
161	$q^* \to q\gamma$	40(45 ± 3)		
GeV	$q^* \to qg$	29(30±2)		
172	$q^* \to q\gamma$	36(33 ± 2)		
GeV	$q^* \to qg$	27(24 ± 2)		

Table 7: Number of excited fermion candidates for the different decay channels in the single production mode. The numbers in brackets correspond to the simulation expectation.

50% to 40% up to $\sqrt{s}$-10 GeV, having then a fast decrease. For excited quarks decaying in quark-photon, it drops from 30% to 25% up to $\sqrt{s}$-10 GeV, and then increases to around 40% due to the inclusion of the h101 topology.

channel	e	μ	τ
$\ell^* \to \ell\gamma$	0(0.03±0.03)	1(0.2±0.1)	1(0.3±0.1)
$\nu^* \to \nu\gamma$	2(0.6±0.1)		

Table 8: Number of excited lepton candidates for the different decay channels in the double production mode. The numbers in brackets correspond to the simulation expectation.

The global efficiency for each channel was then calculated, using the corresponding decay branching ratios(see section 2.3).

For the single production of excited fermions, the upper limits at 95% confidence level on the ratio λ/m_{f^*} (see section 2.3), are a function of the f^* mass. The limits were calculated using a Poisson distribution with background.

Figures 4 and 5 show these limits for the excited leptons assuming $f = f'$ and $f = -f'$ respectively. These limits include the results of the previous analyses at a centre-of-mass energies of 130-136 GeV and 161 GeV [2]. The new data extend the mass region explored up to 172 GeV.

Figures 6(a) and 6(b) shows the limits for the single production of excited quarks assuming a decay branching ratio of 100% into qγ and into qg respectively. The limits were obtained assuming up-type excited quarks. For down-type excited quarks the cross section limits are about 15% lower in the studied mass region.

Using the $\sqrt{s}$=172 GeV and the $\sqrt{s}$=161 GeV data samples, the differential cross section for $e^+e^- \to \gamma\gamma$ was computed at an average centre-of-mass energy of $< \sqrt{s} >= 166.7$

channel	e	μ	τ
$\ell^* \to \ell\gamma$	33	60	30
$\ell^* \to \nu W$	31	48	42
$\ell^* \to \ell Z$	19	38	11
$\nu^* \to \nu\gamma$	42	42	42
$\nu^* \to \ell W$	18	33	15
$\nu^* \to \nu Z$	32	32	32
$q^* \to q\gamma$	20		
$q^* \to qg$	14		

Table 9: Efficiencies for the single production modes at $\sqrt{s} = 172$ GeV. The values were obtained with excited fermion masses of 165 GeV/c^2.

channel	e	μ	τ
$\ell^* \to \ell\gamma$	46	50	45
$\nu^* \to \nu\gamma$	46	46	46

channel	$\sqrt{s}$ =172 GeV	$\sqrt{s}$ =161 GeV
$\ell^* \to \nu W$	17	14
$\nu^* \to \ell W$	12	12

Table 10: Efficiencies for the double production modes at $\sqrt{s} = 161, 172$ GeV. The values were obtained with excited leptons masses of 70 GeV/c^2.

GeV. Since this cross section is to be compared to the lowest order QED prediction, a correction for radiative effects was included. In figure 7 the dots are the measured differential cross section and the solid line is the QED lowest-order prediction. A likelihood fit to the modified angular distribution accounting for the possible excited electron exchange (see section 2.2) was performed. A contour upper limit with 95% confidence level on the ratio $\lambda_\gamma/\mathrm{M}_{e^*}$ as a function of the excited electron mass M_{e^*} was obtained. For the particular value λ_γ=1 of the effective coupling, a limit of M_{e^*} >166 GeV/c^2 was obtained. The dashed line in figure 7 shows the 95% confidence level limit on the modified differential cross section for λ_γ=1.

The 95% confidence level limit obtained on the ratio $\lambda_\gamma/\mathrm{M}_{e^*}$ can extend the limit obtained for the excited electron in the direct search previously reported to a mass region above the kinematic threshold $\mathrm{M}_{e^*} \sim \sqrt{s}$. The combined limit from the direct and indirect searches is shown in figure 8. Up to very close to 172 GeV the result is clearly dominated by the direct production result, while the indirect search allows us to go far beyond this value.

The lower limits at 95% of confidence level on the masses of doubly produced excited

	e^*	μ^*	τ^*	ν^*
$f = f^{'}$	84.6	84.6	84.6	67.9
$f = -f^{'}$	74.6	74.6	74.6	80.1

Table 11: Lower limits (in GeV/c^2) at 95 % confidence level on the excited leptons masses from the double production modes.

leptons are given in table 11. Limits are given for both $f = f'$ and $f = -f'$.

8 Conclusions

DELPHI data corresponding to total luminosities of 10.1 pb^{-1} and 9.7 pb^{-1} at a centre-of-mass energies of 172 GeV and 161 GeV respectively have been analysed, searching for decays of excited fermions involving γ, Z, W and gluon emission. No significant signal was observed.

The search for double production of excited leptons gave the mass limits shown in table 11.

The search for single production of excited fermions gave the limits on the ratio λ/m_f^* shown in Figures 4, 5 and 6.

For excited electrons, this limit was extended in the region above the kinematic threshold using the reaction $e^+e^- \rightarrow \gamma\gamma(\gamma)$ (figure 8). In particular, for an effective coupling value λ_γ=1 M$_{e*}$ >166 GeV/c^2 at 95% confidence level.

Acknowledgements

We are greatly indebted to our technical collaborators and to the funding agencies for their support in building and operating the DELPHI detector. Very special thanks are due to the members of the CERN-SL Division for the excellent performance of the LEP collider.

References

[1] "Searches for new Physics" G.F.Giudice et al., Physics at LEP2, vol. 1, eds. G.Altarelli et al., CERN Yellow Book CERN-96-01 (1996) 463.

[2] DELPHI Coll., P. Abreu et al., Phys. Lett. **B393** (1997) 245;
DELPHI Coll., P. Abreu et al., Phys. Lett. **B380** (1996) 480;
DELPHI Coll., P. Abreu et al., Zeit. Phys. **C53** (1992) 41;
DELPHI Coll., P. Abreu et al., Phys. Lett. **B274** (1992) 230.

[3] K. Hagiwara, S. Komamiya, D. Zeppenfeld, Z. Phys. **C29** (1985) 115.

[4] ALEPH Coll., D. Buskulic et al., Phys. Lett. **B385** (1996) 445;
ALEPH Coll., D. Buskulic et al., Phys. Lett. **B384** (1996) 439;
ALEPH Coll., D. Decamp et al., Phys. Lett. **B250** (1990) 172;
ALEPH Coll., D. Decamp et al., Phys. Lett. **B236** (1990) 511;
H1 Coll., I. Abt et al., Nucl. Phys. **B396** (1993) 3;
L3 Coll., M. Acciarri et al., Phys. Lett. **B377** (1996) 304;
L3 Coll., M. Acciarri et al., Phys. Lett. **B370** (1996) 211;
L3 Coll., B. Adeva et al., Phys. Lett. **B251** (1990) 321;
L3 Coll., B. Adeva et al., Phys. Lett. **B247** (1990) 177;
Phys. Lett. **B250** (1990) 205; Phys. Lett. **B252** (1990) 525;
OPAL Coll., G. Alexander et al., CERN–PPE/96–140, accepted by Phys. Lett. **B**;
OPAL Coll., G. Alexander et al., CERN–PPE/96–138, accepted by Phys. Lett. **B**;
OPAL Coll., G. Alexander et al., Phys. Lett. **B386** (1996) 463;
OPAL Coll., G. Alexander et al., Phys. Lett. **B385** (1996) 433;
OPAL Coll., G. Alexander et al., Z.Phys. C52 (1991) 175;
OPAL Coll., M.Z. Akrawy et al., Phys. Lett. **B257** (1991) 531;
OPAL Coll., M.Z. Akrawy et al., Phys. Lett. **B247** (1990) 448;
OPAL Coll., M.Z. Akrawy et al., Phys. Lett. **B240** (1990) 250;
ZEUS Coll., M. Derrick et al., Z. Phys. **C65** (1994) 627.

[5] F. Boudjema, A. Djouadi and J.L. Kneur, Z. Phys. **C57** (1993) 425.

[6] A. Litke, PhD Thesis Harvard Univ., (1970), unpublished;
D. Treille et al. preprint ECFA 87-108, in: *Compositeness at LEPII* CERN Report 87-08 Vol.2 (1987) 414.

[7] DELPHI Coll., P. Aarnio et al., Nucl. Instr. Methods **A303** (1991) 233;
DELPHI Coll., P. Abreu et al., Nucl. Instr. Methods **A378** (1996) 57.

[8] T. Sjöstrand, Comp. Phys. Comm. **82** (1994) 74;
T. Sjöstrand, Pythia 5.7 and Jetset 7.4, CERN-TH/7112-93.

[9] F.A. Berends, R. Pittau, R. Kleiss, Comp. Phys. Comm **85** (1995) 437.

[10] S. Nova, A. Olchevski and T. Todorov, "TWOGAM, a Monte Carlo event generator for two photon physics", DELPHI Note 90-35 PROG 152.

[11] F.A. Berends, P.H. Daverveldt, R. Kleiss, Comp. Phys. Comm. **40** (1986) 271.

[12] D. Karlen, Nucl. Phys. **B289** (1987) 23.

[13] F. Berends and R. Kleiss, Nucl. Phys. **B186** (1981) 22.

[14] G. Montagna et al., Nucl. Phys. B452 (1996) 161.

[15] S. Catani et al., Phys. Lett. **B269** (1991) 432.

[16] N. Kjaer and R. Moller, "Reconstruction of invariant masses in multi-jet events", DELPHI Note 91-17 PHYS 88.

[17] DELPHI Coll., "Search for charginos, neutralinos and gravitinos at LEP", in preparation.

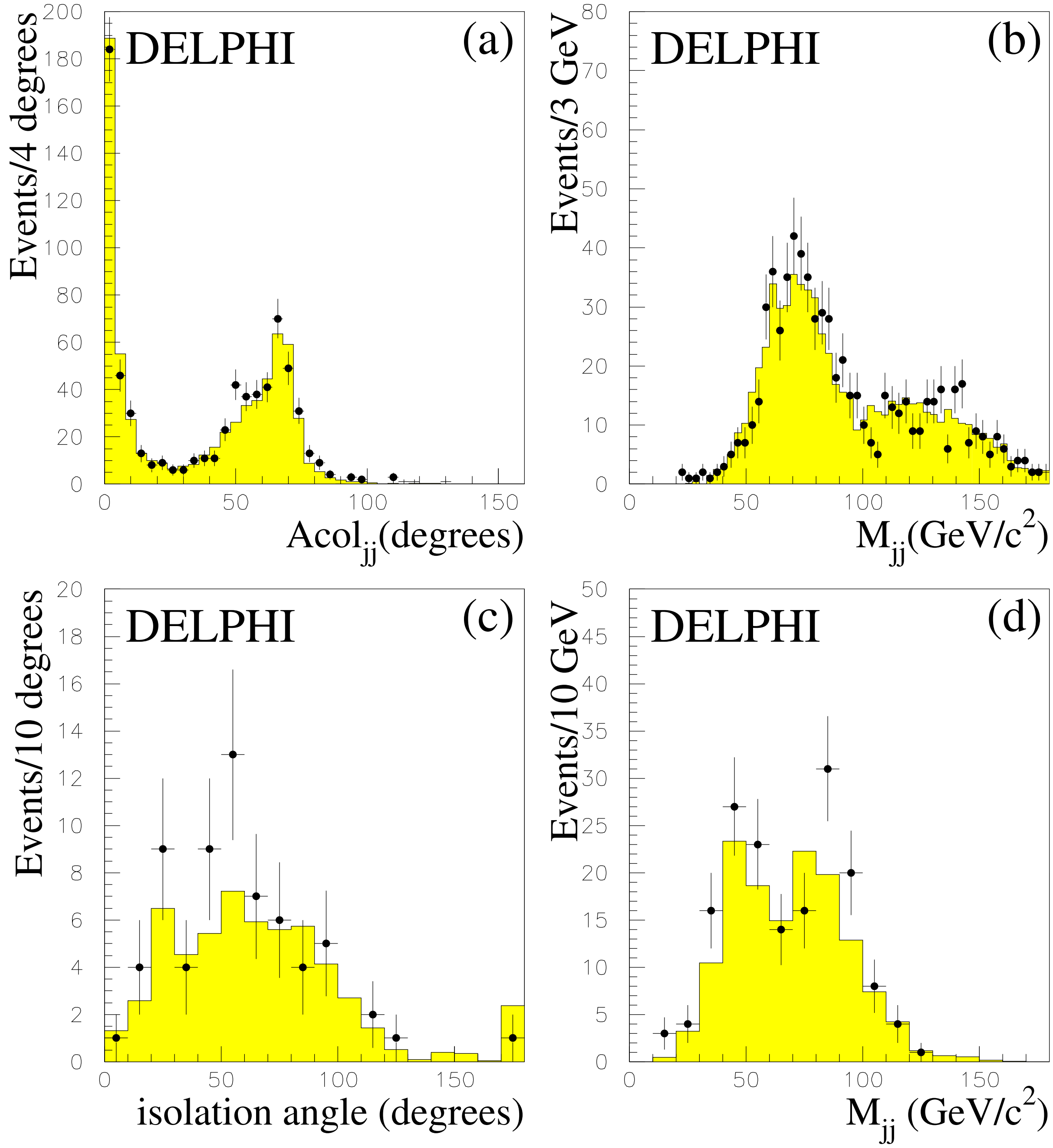

Figure 1: Acollinearity **(a)** and invariant mass**(b)** of the two jets in the h200 topology, isolation angle of the lepton in the h210 topology **(c)**, largest jet-jet invariant mass in the h400 topology **(d)**. The dots show the data and the shaded histogram shows the SM simulation.

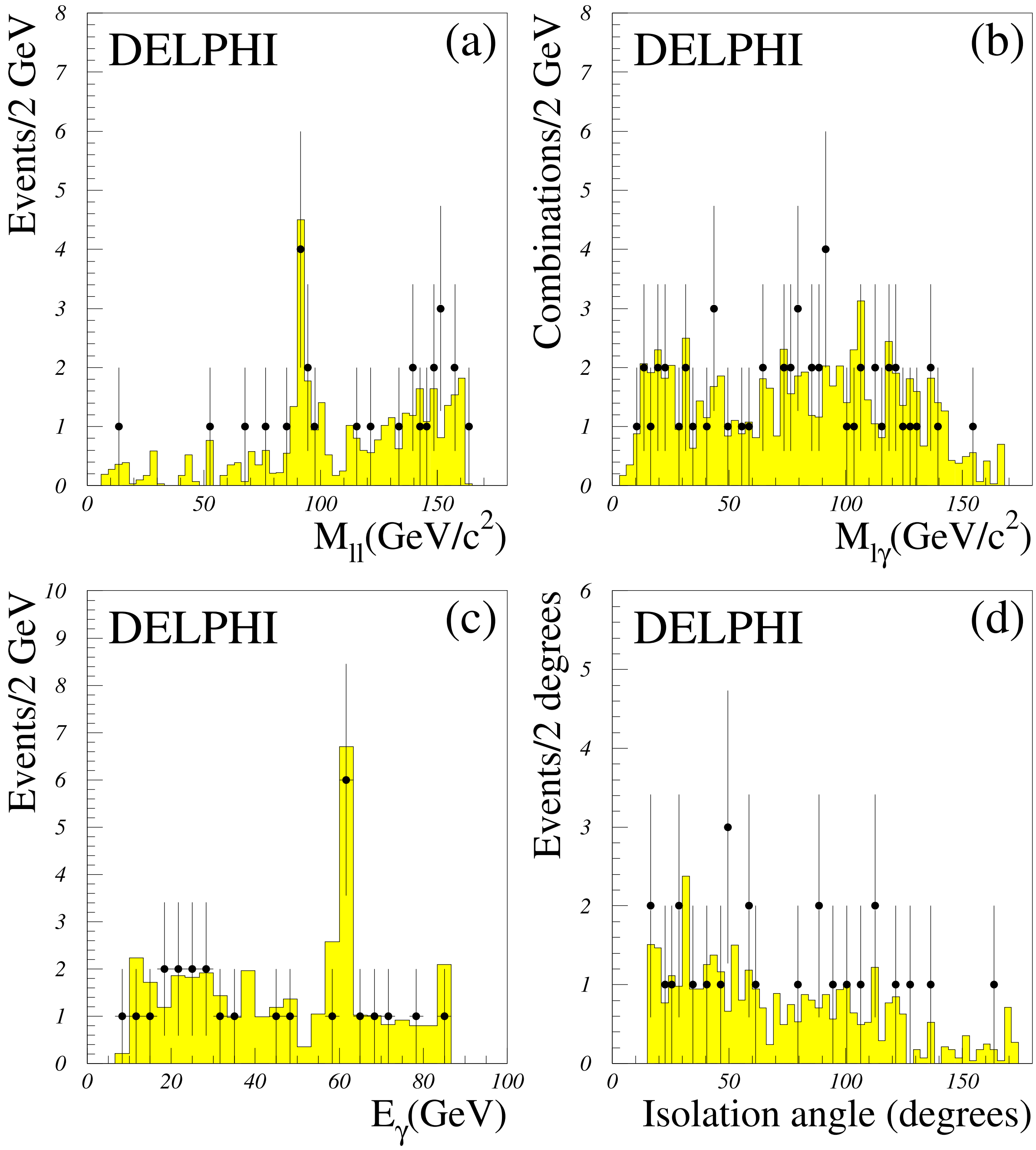

Figure 2: Invariant mass of the two leptons **(a)**, invariant mass of lepton-photon pairs **(b)**, and energy **(c)** and isolation angle **(d)** of the photon, for the ℓ201 sample. The dots show the data and the shaded histogram shows the SM simulation.

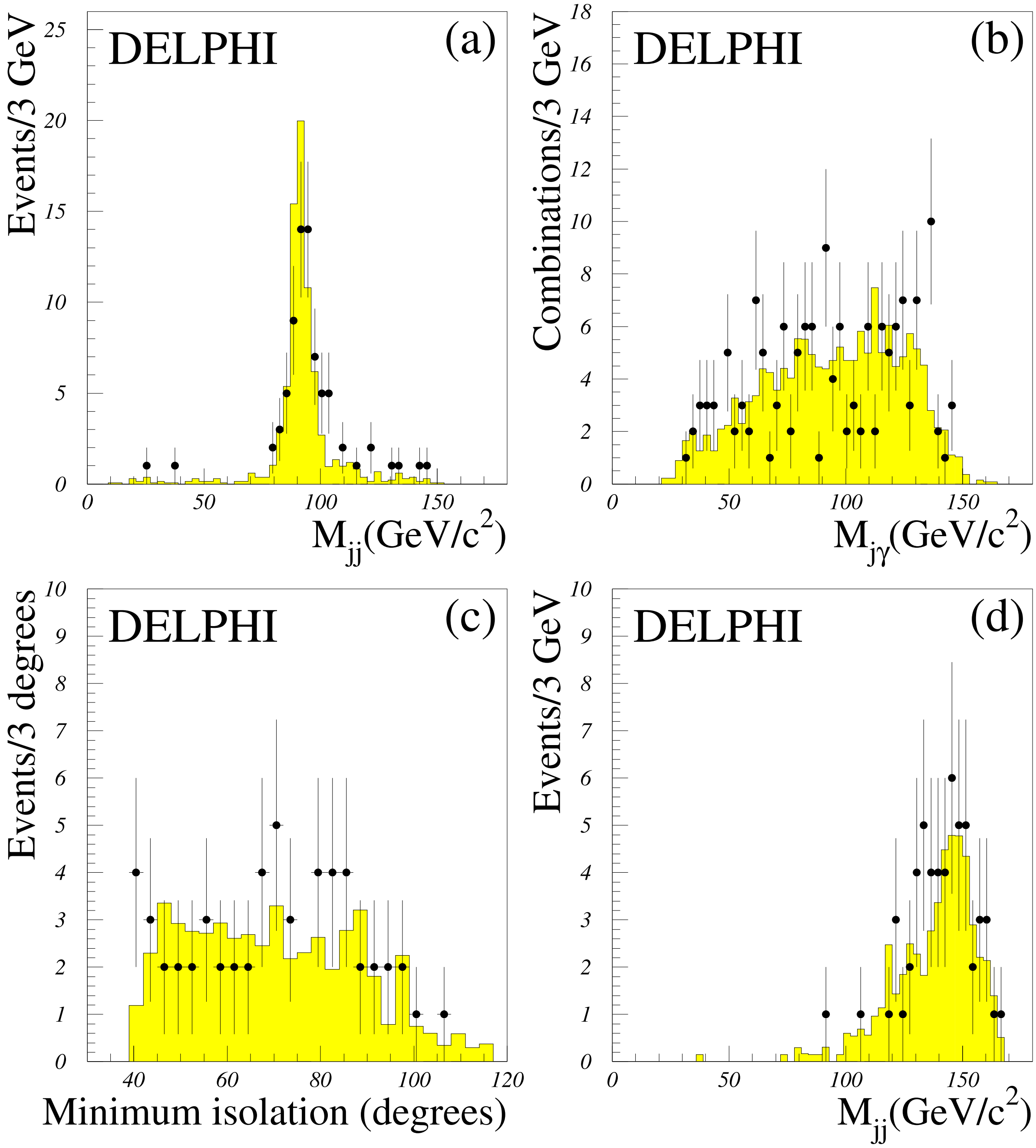

Figure 3: Jet-jet invariant mass (**a**) and jet-photon invariant mass combinations (**b**) for the h201 topology. For the h300 topology, jet isolation angle (**c**) and largest jet-jet invariant mass (**d**). The dots show the data and the shaded histogram shows the SM simulation.

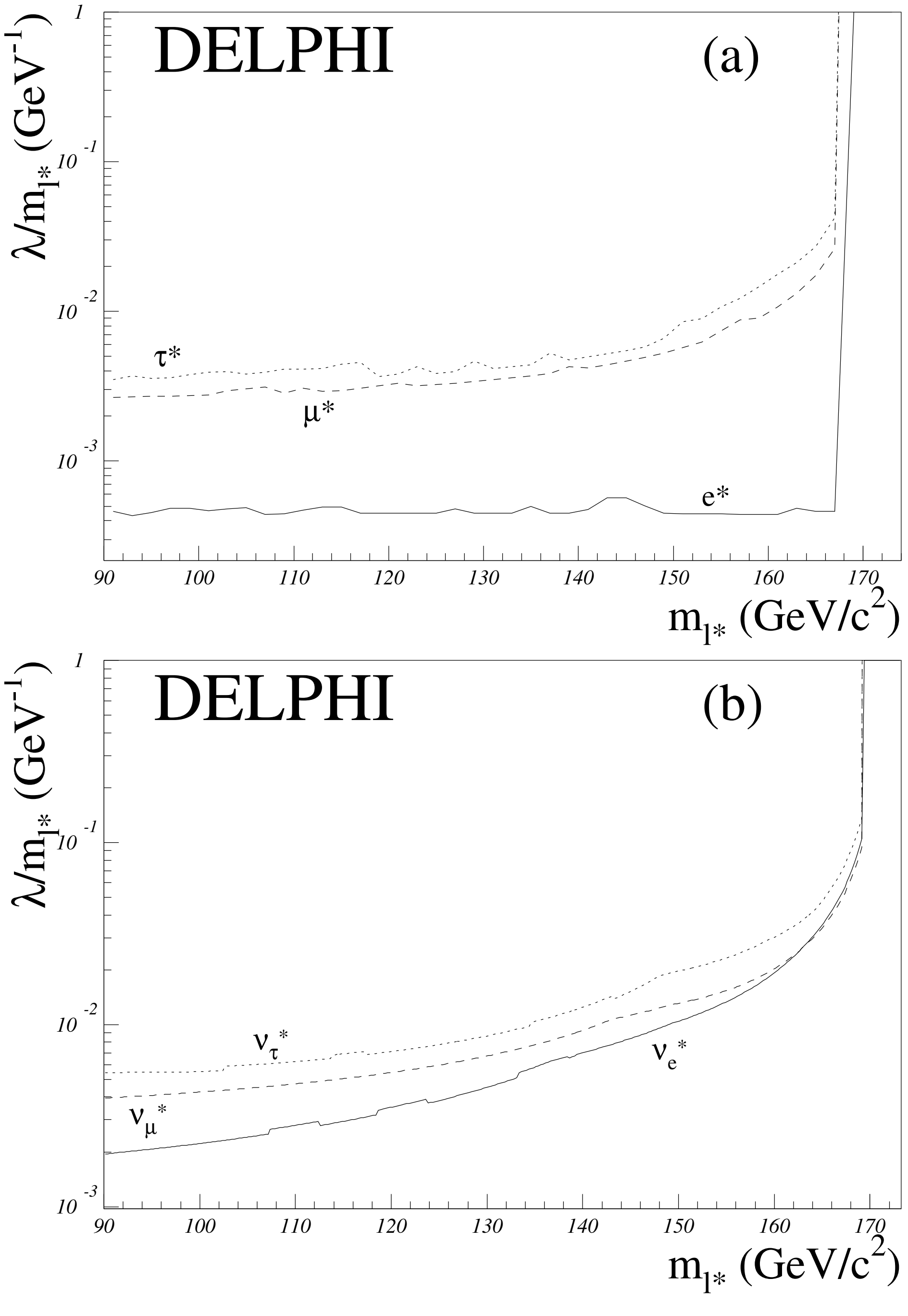

Figure 4: Results on single production of excited charged **(a)** and neutral **(b)** leptons assuming $f = +f'$. The line shows the upper limits at 95% confidence level on the ratio $\lambda/m_{\ell*}$ between the coupling of the excited charged lepton and its mass as a function of its mass.

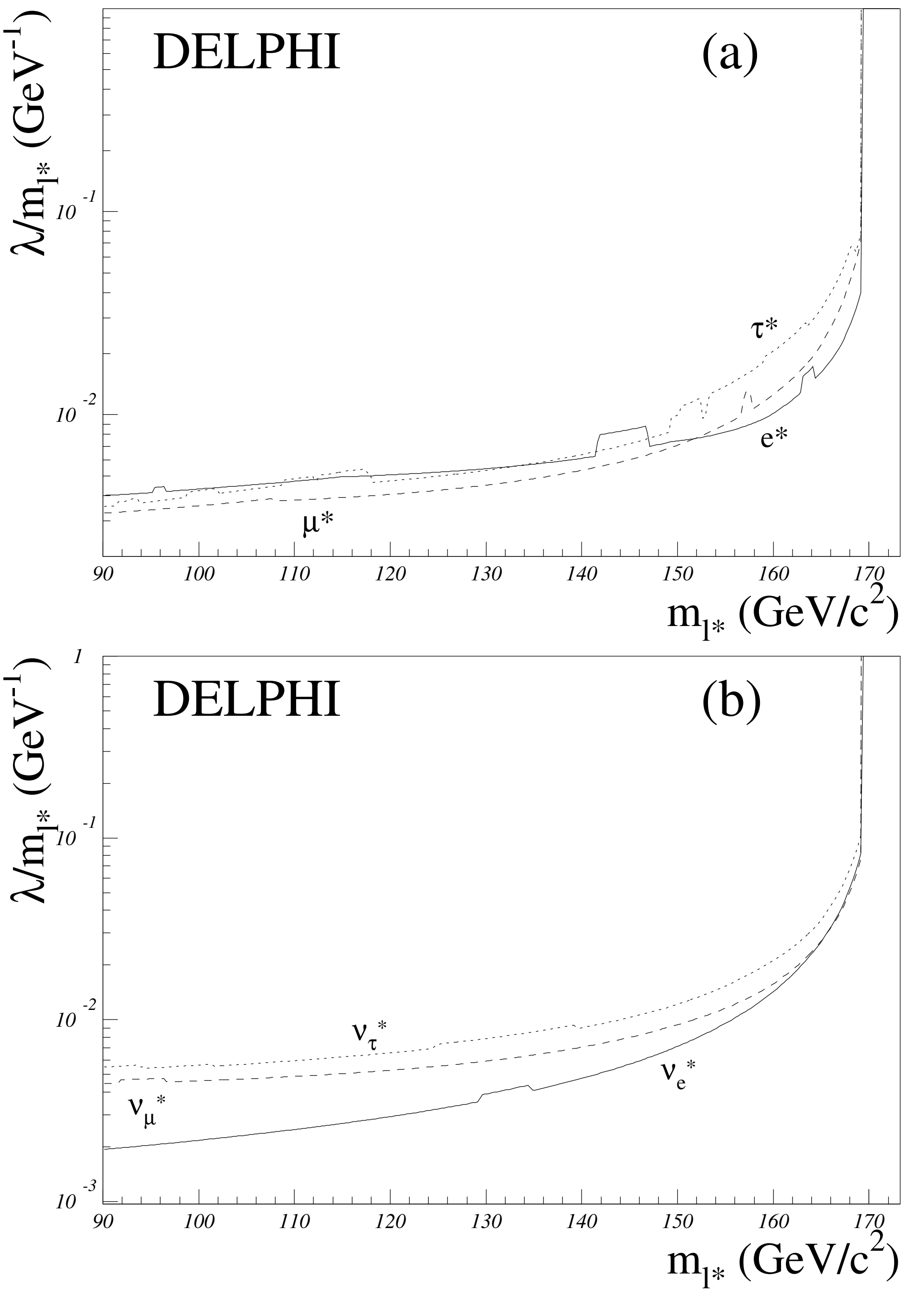

Figure 5: As Fig. 4, but for $f = -f'$.

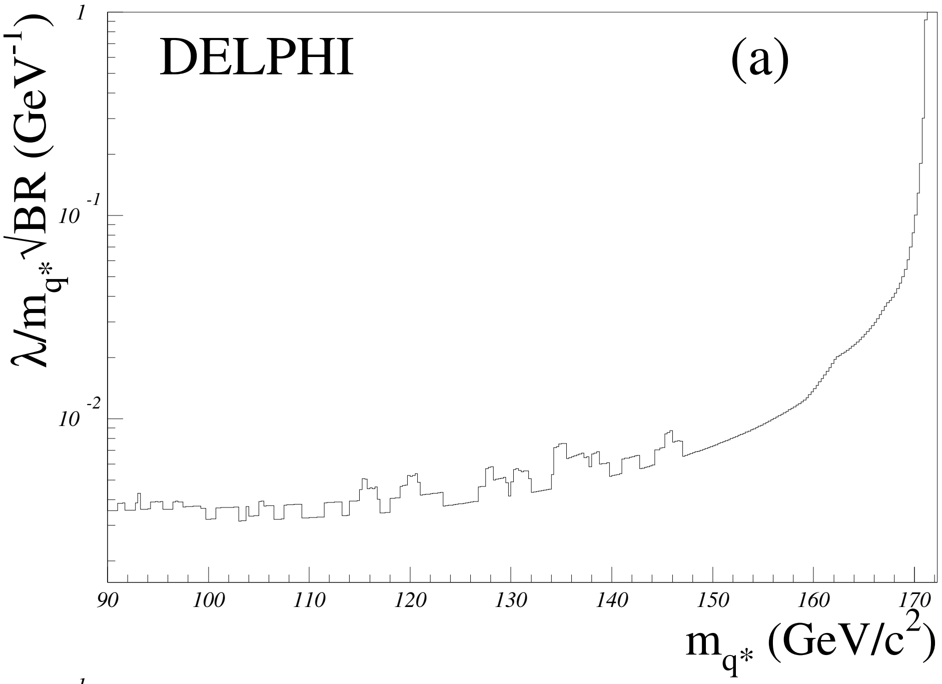

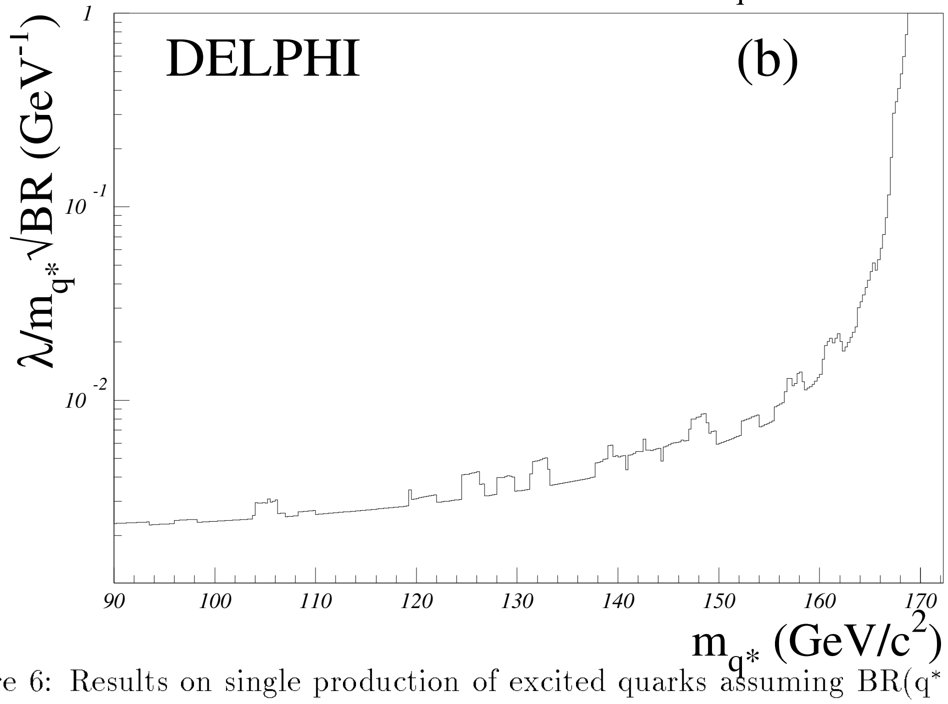

Figure 6: Results on single production of excited quarks assuming BR($q^* \to q\gamma$)=100% (**a**) and BR($q^* \to q\, gluon$)=100% (**b**). The line shows the upper limits at 95% confidence level on the ratio λ/m_{q^*} between the coupling of the excited quark and its mass as a function of its mass

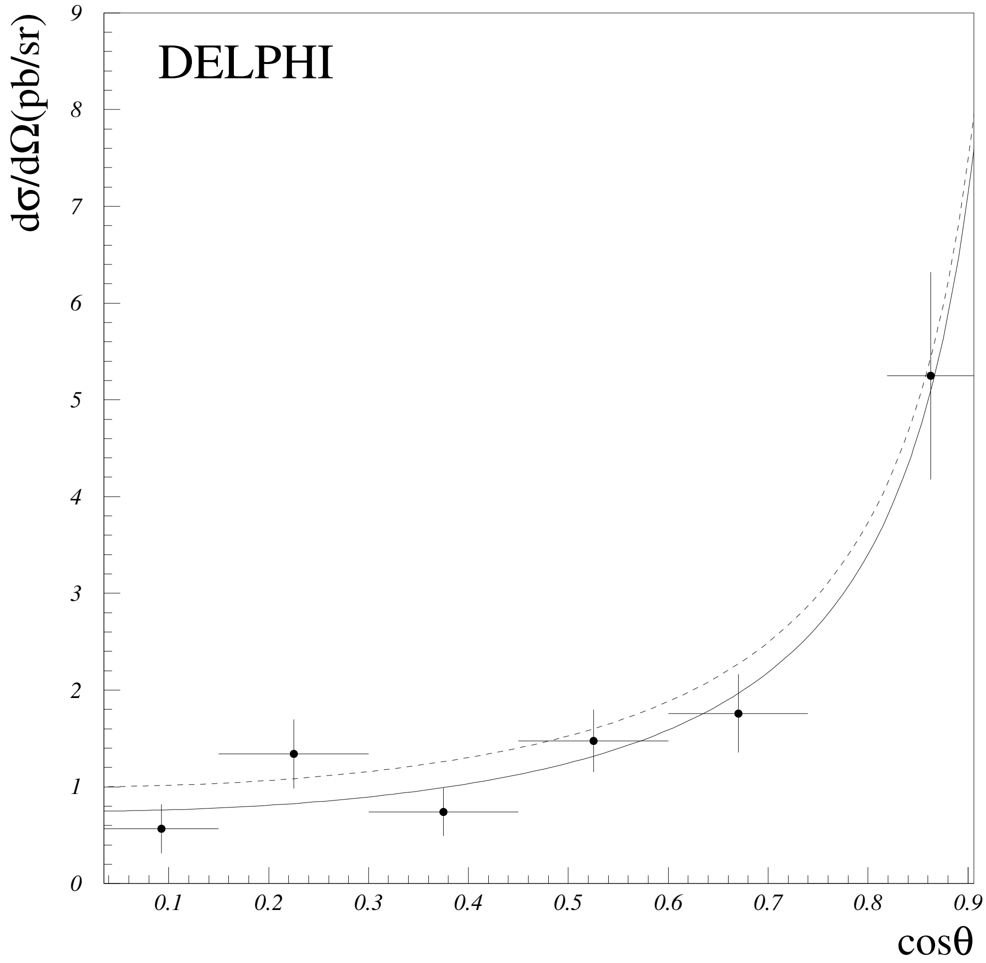

Figure 7: Differential $e^+e^- \rightarrow \gamma\gamma$ cross section at an average center-of-mass energy of $<\sqrt{s}>$=166.7 GeV. The dots are the data, the full line shows the lowest order QED prediction and the dashed line is the 95% confidence level limit on the modified differential cross section for λ_γ=1.

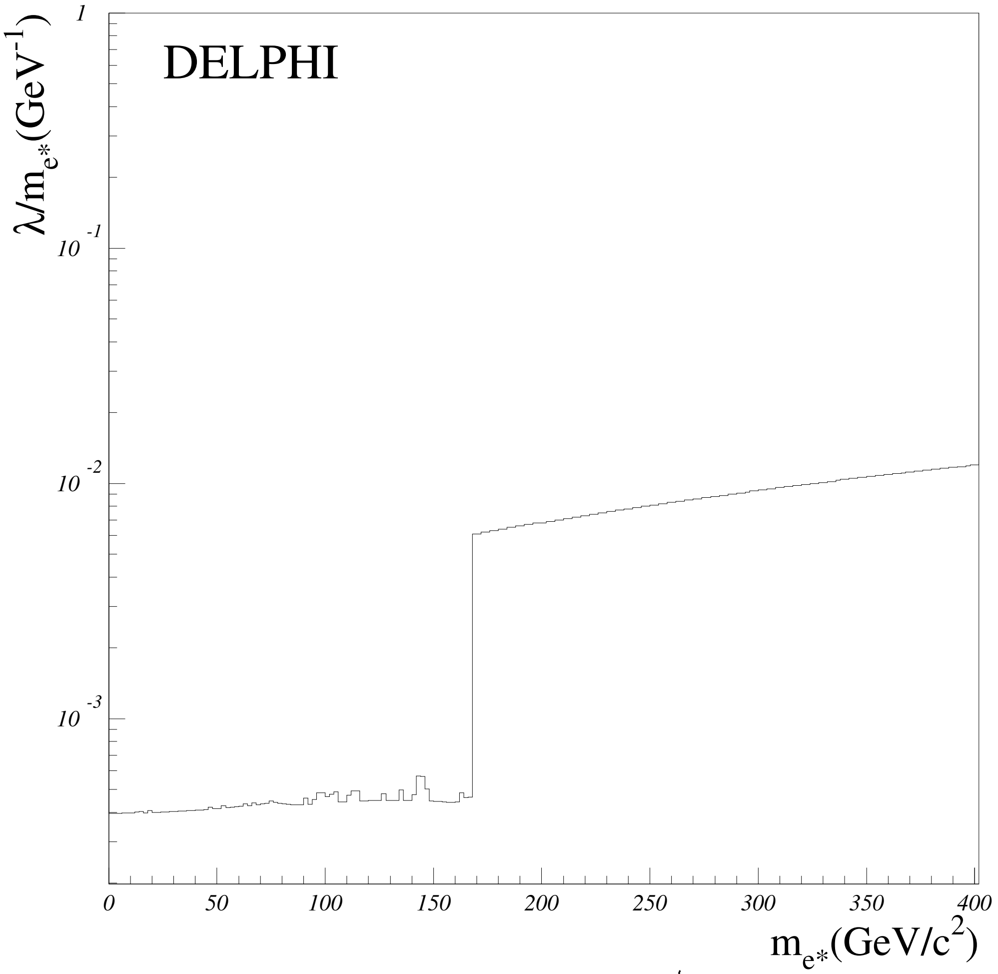

Figure 8: Combined excited electron limits for $f = f'$ from direct and indirect searches. The line shows the upper limits at 95% confidence level on the ratio λ/m_{e^*} between the coupling of the excited electron and its mass as a function of its mass. Up to the kinematic limit the result is dominated by the single production direct search. Above this value the limit is the one coming from the indirect search using $e^+e^- \to \gamma\gamma$.